Dielectric relaxation during physical ageing

E. Schlosser and A. Schönhals
Central Institute of Organic Chemistry, Rudower Chausse 5, O-1199 Berlin, Germany
(Received 18 April 1990; revised 1 August 1990; accepted 17 August 1990)

Isothermal dielectric measurements (frequency range 5×10^{-5}–10^5 Hz) have been carried out on poly(vinyl acetate) above and below the glass transition temperature T_g (from $T_g + 50$ to $T_g - 15$ K) using frequency and time domain measurements. The temperature dependence of such characteristic parameters of the relaxation function as intensity, position, half-width and asymmetry is reported. Near and below the T_g the parameters deviate more from their equilibrium values the lower the temperature. A dramatic change in asymmetry is observed. The deviation of the parameters reflects the influence of physical ageing which can be interpreted according to the concept of sequential relaxation.

(Keywords: dielectric relaxation; Havriliak–Negami function; poly(vinyl acetate); glass transition; physical ageing; sequential relaxation)

INTRODUCTION

It is well known that polymers are not in thermodynamic equilibrium at temperatures below their thermal glass transition temperature, T_g, and thus their properties change with time. This relaxation progresses towards the equilibrium state and is called structural relaxation[1] or physical ageing[2]. It can be demonstrated by measurements of various properties, such as specific volume[1,3], heat content[4], mechanical compliance[2] and dielectric permittivity[5–8].

The important technological significance of physical ageing stems from the fact that the properties of a polymer in the glassy state depend not only on the temperature but also on its thermal prehistory which has been applied from the last quench into the glassy state up to the onset of the testing procedure. Furthermore, there is no generally accepted microscopic interpretation of structural relaxation. Dielectric relaxation measurements above and below the thermal glass transition can give some deeper insight into the processes responsible for structural relaxation.

In this paper the dielectric behaviour of poly(vinyl acetate) (PVAc), a typical amorphous polymer, has been examined for temperatures above and below the T_g in order to characterize the time dependence of physical ageing. In particular, the influence of the ageing time on the frequency position and shape of the dielectric relaxation function has been studied. In comparison with the equilibrium results the mechanism of physical ageing is discussed.

EXPERIMENTAL

The polymer selected for the study was a commercial PVAc obtained from Chemische Werke Buna (Germany). It was synthesized by suspension polymerization and had a number average molecular weight of 67 400 and a weight average molecular weight of 40 800. A $T_g = 311.5$ K was determined by differential scanning calorimetry with a heating rate of 10 K min^{-1}. The sample was cast from a 5 vol% acetone solution onto a 1.5 mm thick copper plate which served as the bottom electrode. The 46 μm thick PVAc film was dried under high vacuum using an annealing programme. The sample was heated in 10 K steps from room temperature to 423 K. At each temperature step the sample was annealed for $\sim$1 h. After drying a silver electrode with a guard ring configuration was evaporated onto the sample.

The copper plate was fixed (with copper powder ensuring good thermal contact) to a disc-shaped glass vessel which was thermostatically controlled by a cryostat to within 0.05 K. The vessel was mounted in a thermally isolated chamber. Since PVAc is known[6] to absorb $\sim$4 wt% water as 'bound water', causing the T_g to decrease from 43 to 18°C, the air in the chamber was dried with silica gel. The measurements were reproducible throughout the study, and there was no change in T_g due to change in water content.

Above T_g the complex permittivity, i.e.

$$\varepsilon^*(\omega) = \varepsilon'(\omega) - i\varepsilon''(\omega) \qquad (1)$$

where ε' is the permittivity, ε'' is the loss factor, and $\omega = 2\pi f$ where f = frequency, was measured in the frequency range 1–10^5 Hz using bridge methods described previously[9,10].

Near the T_g the dielectric relaxation times were of the magnitude of minutes or hours. This meant that the alternating current measurements were time consuming. Therefore dielectric measurements in the time domain were preferred. The relaxation behaviour was measured by the density of the depolarization current $j(t)$ for a field E_0 which was switched off at time $t = 0$:

$$j(t)/E_0\varepsilon_a = \dot{\varepsilon}(t) \qquad t > 0 \qquad (2)$$

where the relaxation function $\dot{\varepsilon}(t)$ is the time derivative of the time-dependent dielectric permittivity $\varepsilon(t)$ and ε_a is the permittivity of free space.

A block diagram of the depolarization measuring system employed is shown in *Figure 1*. With the system $\dot{\varepsilon}(t)$ could be determined from 0.5 to 5×10^4 s.

It was convenient to discuss the function $t\dot{\varepsilon}(t)$ instead

0032-3861/91/122135-06
© 1991 Butterworth-Heinemann Ltd.

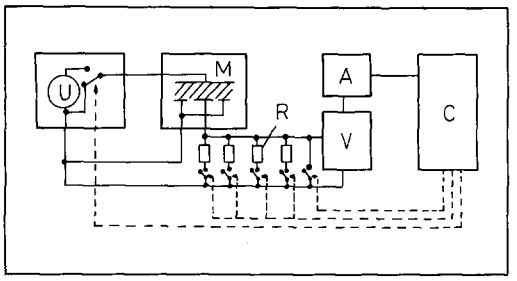

Figure 1 Depolarization measuring system: U, polarization voltage, switched at $t = 0$; M, measuring chamber with sample, temperature controlled by cryostat; V, vibration reed electrometer; A, 12 bit analog digital converter; C, computer for controlling the sampling time from 0.5 to 5×10^4 s, for storage and evaluation of the data; R, resistors to adapt the sensitivity of the electrometer; ---, computer controlling lines

of $\dot{\varepsilon}(t)$ because $t\dot{\varepsilon}(t)$ exhibited a maximum analogous to that of $\varepsilon''(\omega)$ (cf. ref. 11).

Below T_g the relaxation function depended on the thermal prehistory. For this reason a well defined thermal treatment was used. We applied the following procedure:

1. Polarization (with $E \approx 2 \times 10^4$ V cm^{-1}) in thermodynamic equilibrium (60°C) for 300 s (α process fully stimulated).
2. Cooling (with applied field) to the temperature of measurement T_M by replacing the cryostat with a bath temperature of 60°C with one with a bath temperature of T_M. This resulted in an exponential temperature decay with a time constant of ~ 20 s.
3. Annealing (with applied field) at T_M for a time t_e (elapsed time from the beginning of cooling). Three logarithmically equidistant times, $t_e = 300$, 1600 and 8530 s, were used.
4. The depolarization experiment was started after time t_e had passed.

The introduction of t_e meant that the structural relaxation proceeds during the time $t_e + t$ whereas the dielectric response is recorded only during time t.

EVALUATION

It is adequate for our problem to discuss the dielectric properties in the time domain (using the function $t\dot{\varepsilon}(t)$). For this purpose the measurements obtained in the frequency domain were evaluated by fitting the imaginary part of the model function of Havriliak and Negami[12] (HN function) and an additive term[13] accounting for direct current conductivity σ

$$\varepsilon^*(\omega) - \varepsilon_\infty = \Delta\varepsilon[1 + (i\omega\tau_0)^\beta]^{-\gamma} + \sigma/(\omega\varepsilon_a) \qquad 0 < \beta,\ \beta\gamma < 1 \quad (3)$$

to the experimental data ε''_ν. Here $\Delta\varepsilon$ is the intensity, τ_0 the position parameter, β, γ are shape parameters, and $\varepsilon_\infty = \varepsilon'(\omega)$ for $\omega \gg \tau_0^{-1}$. Subsequently the function $t\dot{\varepsilon}(t)$ was calculated by Fourier-transform of the HN function:

$$t\dot{\varepsilon}(t) = t\Delta\varepsilon \int_0^\infty [1 + (i\omega\tau_0)^\beta]^{-\gamma} e^{i\omega t}\, d\omega \quad (4)$$

With respect to the time domain data the HN parameters are obtained directly[13] by a computer least squares fit of equation (4) to the data $\dot{\varepsilon}_\nu$.

If the measurement of the relaxation function required data determination in the frequency and time domain a combined evaluation procedure was used[13]. An example is given in *Figure 2*. However, the shape of the measured function $t\dot{\varepsilon}(t)$, if influenced by structural relaxation, differs from the shape predicted by the HN function. This is reflected by reduced accuracy of fitting (measured by the sum of least squares) to a small extent compared with the equilibrium results. For clarity it is advantageous for a discussion of the shape of the relaxation function $t\dot{\varepsilon}(t)$ to use shape parameters which are defined independently of the HN function. These are the position parameters t_m, t_1 and t_2 due to the maximum and half-height of the function $t\dot{\varepsilon}(t)$ at short and long times, respectively (cf. *Figure 3*):

$$1/2t_m\dot{\varepsilon}(t_m) = t_1\dot{\varepsilon}(t_1) = t_2\dot{\varepsilon}(t_2) \qquad t_1 < t_m < t_2 \quad (5)$$

Also the half-width, b_t, and the asymmetry, u_t, were used which characterized the shape more directly:

$$b_t = b_1 + b_2 \qquad u_t = \frac{b_1 - b_2}{b_t} \quad (6)$$

with

$$b_1 = \log t_m - \log t_1 \qquad b_2 = \log t_2 - \log t_m$$

DISCUSSION

The results of this study are presented in *Figures 4–6*. *Figure 4* shows the characteristic times (log scale) $\log t_1$, $\log t_m$ and $\log t_2$ *versus* $10^3/T$. For the sake of clarity the t_1 and t_2 values for $t_e = 1600$ and 8530 s were omitted.

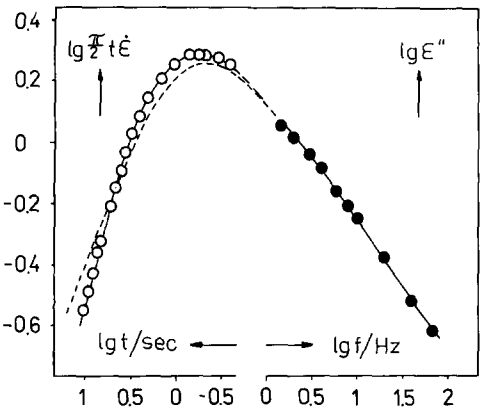

Figure 2 Data measured in frequency (●) and time (○) domain at $T = 46.9$ °C. Fit of the data due to the HN parameters: $\Delta\varepsilon = 6.33$; $\beta = 0.848$; $\gamma = 0.503$; $\log \tau_0 = 0.181$; ---, continued curve of the fit in the frequency and time domain, respectively

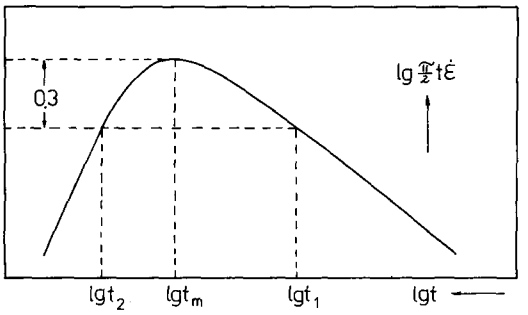

Figure 3 Definition of the characteristic times t_m, t_1 and t_2

The shape parameters b_t and u_t are shown in *Figure 5*.

In *Figure 6* the temperature dependence of the HN parameters $\Delta\varepsilon$, β and of the product $\beta\gamma$ is shown, the latter because it is physically more relevant than γ as found from theoretical considerations[14]. A graph of $\log \tau_0$ *versus* $10^3/T$ is not presented because such a plot does not provide any more information than the plot of $\log t_m$ *versus* $10^3/T$.

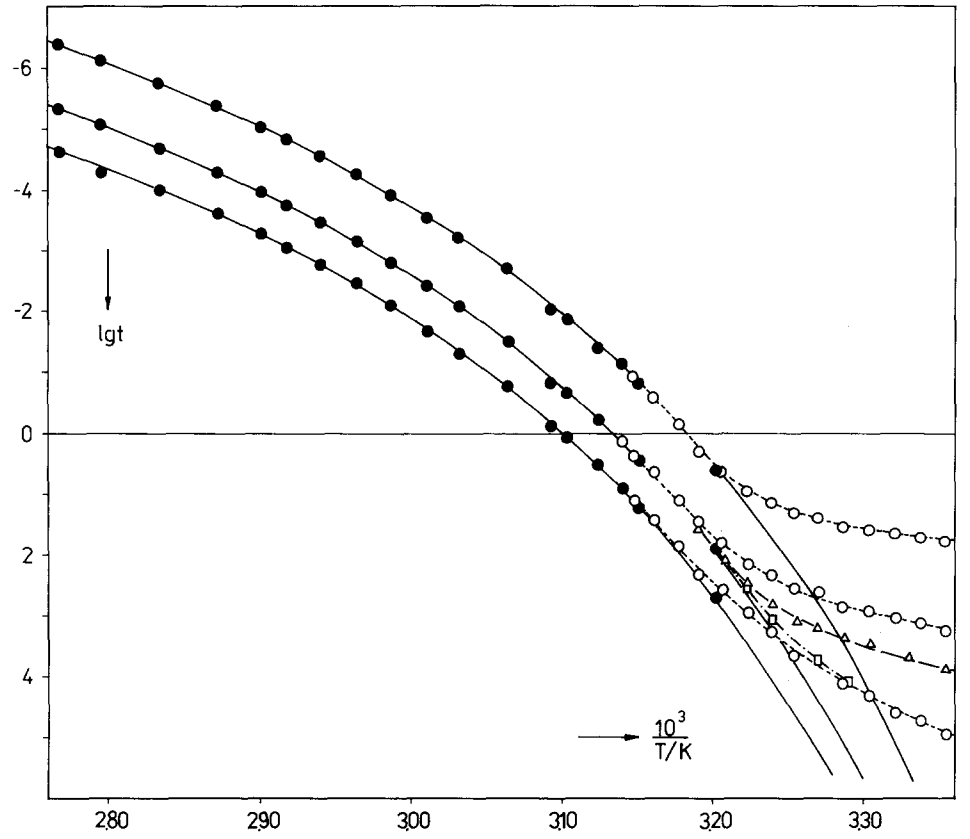

Figure 4 Plot of the characteristic times *versus* $10^3/T$: ———, dependence according to Vogel equation; – – – –, t_e = 300 s; — — —, t_e = 1600 s; — · —, t_e = 8530 s. Symbols of measured values: ●, equilibrium; ○, t_e = 300 s; Δ, t_e = 1600 s; □, t_e = 8530 s

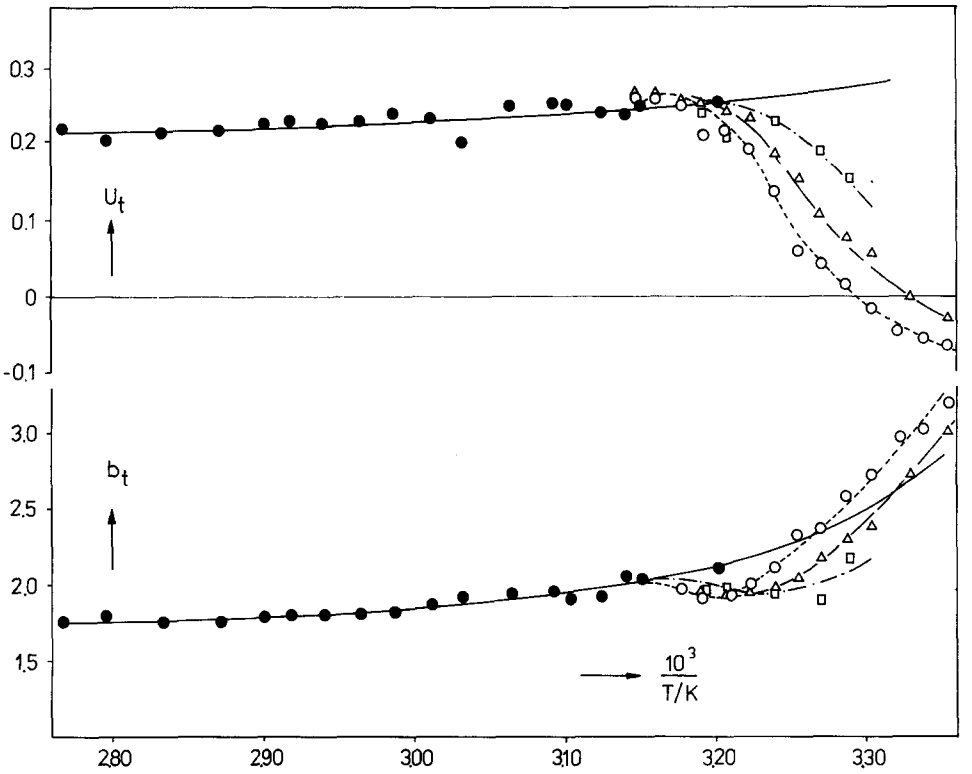

Figure 5 Plot of u_t and b_t *versus* $10^3/T$: ———, calculated according to equation (6) using the Vogel equations for t_m, t_1 and t_2. For symbols see *Figure 4*

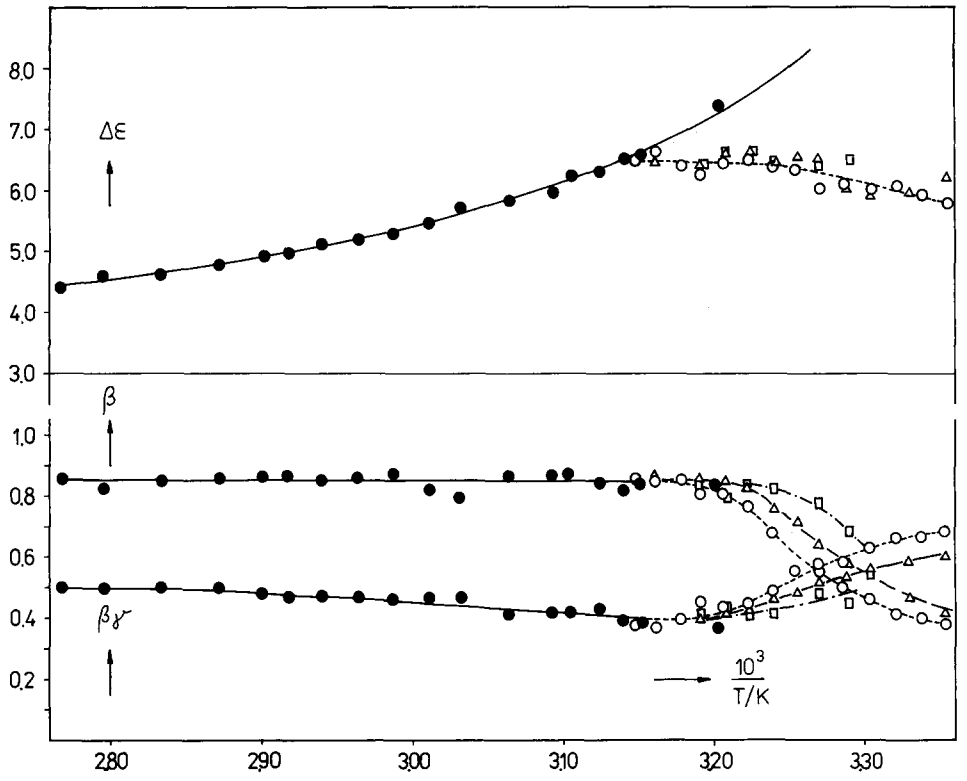

Figure 6 Plot of $\Delta\varepsilon$, β and $\beta\gamma$ *versus* $10^3/T$: ———, dependence according to equation (8). For symbols see *Figure 4*

Table 1 Parameters for the Vogel equations

i	Log $t_{i,\infty}$	$T_{i,0}$ (K)	A_i (K)
1	−12.50	269.3	563.1
m	−11.45	270.8	554.8
2	−10.75	271.5	549.0

Equilibrium properties

The temperature dependence of the log t_m values determined at equilibrium could be fitted closely by the well known Vogel–Fulcher equation[15] (or the equivalent WLF equation[16]):

$$\log t_m = \log t_{m,\infty} + \frac{A_m}{T - T_{m,0}} \tag{7}$$

The parameters are given in *Table 1*.

It was established[17] that the temperature dependence of log t_1 and log t_2 also fit Vogel-type functions with the same $T_{i,0}$. Careful examination of the measurements showed that Vogel-type equations are valid, but with a separation of the $T_{i,0}$ values. Additionally, separate values of $t_{i,\infty}$ were observed. The constants determined are given in *Table 1*. The solid lines in *Figure 4* are the curves calculated using these parameters. The separation of $t_{i,\infty}$ and $T_{i,0}$ shows a characteristic arrangement. This can be understood in terms of a model of dielectric relaxation[14] published recently. As regards $t_{i,\infty}$ in the limit of high temperatures this model predicts a special type of molecular motion connected mainly with local chain dynamics which leads to values of $b_t = 1.16$ and $u_t = 0.27$, corresponding approximately to the measured values $b_t = 1.7$ and $u_t = 0.18$.

The temperature T_0 can be interpreted as a measure of the cooperativity of the molecular motion. Local molecular motions have low T_0 values whereas highly cooperative motions have higher values. In the analysis the lowest T_0 belongs to the short time t_1 and the highest value of T_0 belongs to the longer time t_2 (cf. *Table 1*). In the model the short time tail of the relaxation function is related to more local motions whereas the long time tail is connected to more cooperative motions[14]. Thus the observed arrangement of T_0 values is further evidence for this model.

As for most polymers b_t and u_t decrease gradually with $1/T$ (*Figure 5*). (The solid lines in *Figure 5* are calculated using the Vogel equations for t_1, t_m and t_2.)

Considering the HN shape parameters (*Figure 6*), β is nearly constant over the whole temperature range and $\beta\gamma$ decreases gradually with $1/T$. The limiting value 0.5 for high temperatures was also predicted by our model[14].

The temperature dependence of the intensity $\Delta\varepsilon$ is shown in *Figure 6*. It is obvious that the dependence does not obey the frequently used $1/T$ law[18], but it can be described by a Vogel-like temperature dependence:

$$\Delta\varepsilon(T) = 2.85 + \frac{122.7\ \text{K}}{T - 285.2\ \text{K}} \tag{8}$$

Moreover, it is remarkable that the fit with $T_0 = 285.2$ K led to a value which is in the vicinity of $T_{m,0} = 270.8$ K as determined for the temperature dependence of $t_m(T)$. A more refined discussion of this result will be presented elsewhere[19].

Recently Nozaki and Mashimo have studied the dielectric behaviour of PVAc in equilibrium over a wide temperature and frequency range[20] and used the HN equation for the representation of their data. They found that 15 K above the reported T_g a drastic change in the temperature dependence of the HN parameters takes

place (cf. Figures 7 and 8 of ref. 20). This result cannot be confirmed by our study. On the contrary, we found that from high temperatures down to temperatures near T_g (as long as the equilibrium state is attained by annealing) all parameters obey monotonic temperature dependences which can be described by proper mathematical functions. For instance, the Vogel equations for the characteristic times are valid in equilibrium at all temperatures.

Non-equilibrium properties and the mechanism of physical ageing

Let us consider the temperature dependence of the maximum position t_m (*Figure 4*). Obviously, below T_g the t_m values are smaller than predicted by the extrapolated Vogel curve. This means that the equilibrium state could not be reached within t_e and the time scale of measurement at these temperatures. The amount of the deviation increases with decreasing temperature and for shorter t_e.

The temperature dependence of t_m under non-equilibrium conditions is characterized by a lowering of the apparent activation energy ΔU when compared with that due to equilibrium conditions at the same temperature. For $T \ll T_g$ a nearly constant value of $\Delta U \approx 100\ \text{kJ mol}^{-1}$ can be estimated for $t_e = 300$ s.

Gradually greater values of ΔU are observed for increased t_e values and for shorter t_e values the activation energy of the β process ($\Delta U \approx 42\ \text{kJ mol}^{-1}$)[21] seems to be approached. However, the pre-exponential factors (obtained by extrapolation of the respective Arrhenius plot for $T \to \infty$) are far beyond any physical meaning. Therefore it must be concluded that the processes responsible for physical ageing are not solely thermally activated and the Arrhenius equation is not an appropriate description.

Comparing the three characteristic times t_1, t_2 and t_m for one t_e (e.g. for $t_e = 300$ s in *Figure 4*) one notices with decreasing temperature at first a deviation from equilibrium for t_2, and then for t_m and t_1. This means that the shorter relaxation times reach equilibrium faster than the longer times.

With respect to the shape of the relaxation curves this behaviour is more distinctly reflected by the temperature dependence of the half-width b_t and asymmetry u_t; b_t shows a broad minimum compared to the equilibrium curve around T_g (cf. *Figure 5*) reflecting the fact that in this temperature range the short time tail of the relaxation curve reaches the equilibrium state faster than the long time tail. The strong increase in b_t at lower temperatures indicates that neither the short time tail nor the long time tail reach their equilibrium state. At the same time u_t decreases and becomes negative at low temperatures, exhibiting an asymmetry for $u_t < 0$ which does not occur at measurements in equilibrium.

Physical ageing is frequently described as a simple uniform shift of the main relaxation process to longer times with increasing ageing times[2]. Using this concept the different behaviour of the characteristic times (minimum of half-width) cannot be understood.

However, this behaviour can be discussed applying the idea of sequential relaxation as introduced by McCrum[22] and further discussed elsewhere[23]. The key point of this analysis[23] is the idea that physical ageing cannot simply be treated as a continuation of the glass transition. Rather it has been argued that between the β relaxation and the glass transition there exists a spectrum of motional processes which are responsible for physical ageing. These molecular motions can be characterized by spatial correlation length which increases with increasing ageing time from a value due to local motion (with an apparent activation energy near that of β relaxation) to one due to cooperative motion (with greater apparent activation energy).

This is supported by experimental results. The relatively low apparent activation energy for short ageing times indicates that the spatial extent of the molecular motion is small (in comparison with the glass transition) in the first stage of physical ageing. The increase of the apparent activation energy with increasing ageing time shows that the respective molecular movement becomes more complex with further ageing. Accordingly the apparent activation energy increases also with increasing characteristic time. (Compare the value of the apparent activation energy for t_1, which is comparable with that of the β process, and the higher value for t_2.)

Of course, these results are also reflected by the temperature dependence of the HN parameters β and $\beta\gamma$ (cf. *Figure 6*), but the parameters cannot be interpreted directly as is possible in the equilibrium case[14].

As expected, around T_g the intensity $\Delta\varepsilon$ also shows deviation from equilibrium behaviour and reaches a nearly constant level (cf. *Figure 6*), slightly decreasing with lower temperatures. This behaviour can be understood taking into consideration the thermal prehistory. The intensity related to the polarization state depends on the molecular motion responsible for the orientation and reorientation processes which changes strongly with temperature. For temperatures higher than T_g the equilibrium state of polarization can be reached during the ageing time which is needed for adjusting to T_m. If around T_g the molecular motion responsible for the glass transition freezes then a freezing of the polarization state is also obtained. Clearly only this polarization state can be released during the following depolarization measurement and leads to a nearly constant level of $\Delta\varepsilon$. The slight decrease in $\Delta\varepsilon$ at lower temperatures can be discussed in two ways. (1) Because an exponential cooling regime is used the velocity of passing through the glass transition increases with the absolute height of the temperature step. This means that at low temperatures a lower polarization state is gradually obtained. (2) The measuring time of the spectrometer is limited to 5×10^4 s. For this reason the influence of ageing on the long time tail of the relaxation curve could not be determined exactly and this would lead to an underestimation of $\Delta\varepsilon$.

ACKNOWLEDGEMENTS

We thank Mrs R. Merker for carefully performing the dielectric experiments and Mr V. Zschuppe for the determination of the glass transition temperature by differential scanning calorimetry.

REFERENCES

1 Kovacs, A. G. *Fortschr. Hochpolym. Forschung* 1963, **3**, 394
2 Struik, L. C. E. 'Physical Ageing in Amorphous Polymers and Other Materials', Elsevier, Amsterdam, 1978
3 Greiner, R. and Schwarzel, F. R. *Rheol. Acta* 1984, **23**, 378

4 Marshal, A. S. and Petrie, S. E. B. *J. Polym. Sci., Polym. Symp.* 1975, **95**, 245
5 Uchidoi, M., Adachi, K. and Ishida, Y. *Polym. J.* 1978, **10**, 161
6 Bair, H. E., Johnson, G. E. and Anderson, E. W. *Am. Chem. Soc., Div. Polym. Chem.* 1980, **21**, 21
7 Matsuoka, S., Williams, G., Johnson, G. E. and Anderson, E. W. *Macromolecules* 1985, **18**, 2652
8 Heinrich, W. and Stoll, B. *Progr. Colloid Polym. Sci.* 1988, **78**, 37
9 Schlosser, E. *Plaste. Kautschuk* 1962, **9**, 582
10 Schlosser, E. and Horn, G. Z. *Exp. Techn. Physik* 1963, **11**, 145
11 Hamon, B. V. *Proc. Inst. Electr. Eng. Part IV* 1952, **99**, 151
12 Havriliak, S. and Negami, S. *J. Polym. Sci., Polym. Symp.* 1966, **14**, 99
13 Schlosser, E. and Schönhals, A. *Colloid Polym. Sci.* 1989, **267**, 963
14 Schönhals, A. and Schlosser, E. *Colloid Polym. Sci.* 1989, **267**, 125
15 Vogel, H. *Physik. Z.* 1921, **22**, 645
16 Williams, M., Landel, R. F. and Ferry, J. D. *J. Am. Chem. Soc.* 1955, **77**, 3701
17 Schlosser, E. *Polym. Bull.* 1982, **8**, 416
18 Jonscher, A. K. 'Dielectric Relaxation in Solids', Chelsea Dielectrics Press, London, 1983, p. 25
19 Schönhals, A. and Schlosser, E. in preparation
20 Nozaki, R. and Mashimo, S. *J. Chem. Phys.* 1987, **87**, 2271
21 Ishida, Y., Matsuo, M. and Yamafuji, K. *Kolloid Z. Z. Polym.* 1962, **180**, 108
22 McCrum, N. G. *Polym. Commun.* 1984, **25**, 2
23 Schönhals, A. and Donth, E. *Acta Polym.* 1986, **37**, 475